Dosimetric Framework for Therapeutic Alpha-Particle Emitters

John C. Roeske and Thomas G. Stinchcomb

Departments of Radiation and Cellular Oncology, The University of Chicago; and Department of Physics, DePaul University, Chicago, Illinois

Alpha-particle emitters are currently being considered for the treatment of metastatic disease. However, the dosimetry of alpha-particle emitters is a challenge because the dimensions of subcellular targets (e.g., the cell nucleus) are of the same order of magnitude as the range of the particle. Hence, a single dose value is often not representative of the dose delivered to a cell population. Here, we propose a dosimetry system that combines the calculational ease of the Medical Internal Radiation Dosimetry (MIRD) system with the additional information provided by microdosimetry. **Methods:** Beginning with the microdosimetric, single-event specific-energy spectrum, we derived expressions for the first and second moments. Using the MIRD S-factor along with these moments, we determined not only the mean absorbed dose but also the s.d. and the fraction of cells receiving zero (or any number of) hits. **Results:** Using the formalism developed here, we have generated tables for a simple example to demonstrate the use of this method. **Conclusion:** We have developed a formalism for the rapid determination of not only the mean absorbed dose but also the s.d. and fraction of cells receiving zero hits. These parameters are potentially useful in analyzing the biological outcome for cells exposed to alpha-particle irradiation.

Key Words: alpha-particle emitters; dosimetry; microdosimetry; radiation therapy

J Nucl Med 1997; 38:1923–1929

Alpha-particle emitters are currently being considered for several clinical trials in the treatment of metastatic disease (*1–12*). The advantage of using alpha particles is their short range (50–90 μm), high linear energy transfer (LET) and independence from dose rate and oxygen effects (*13*). A major disadvantage is the difficulty in measuring and/or modeling the spatial and temporal distribution of the source activity. Moreover, the dosimetry of alpha-particle emitters is a challenge because the dimensions of subcellular targets (e.g., cell nuclei) are of the same order of magnitude as the range of the particles.

For alpha-particle irradiation, the targets (cell nuclei or other specified volumes) do not all receive the same dose. Rather, they receive a distribution of doses over a range that, in some cases, can be quite wide (*14*). Additionally, some targets may receive no dose if an alpha particle does not hit them. This concept is illustrated schematically in Figure 1. Consider cells that are irradiated in a uniform solution of alpha-particle emitters. The tracks of the alpha particles (arrows) show that, whereas, some cells may receive multiple hits, and others receive few, if any, hits. (Here, the terms hit and event are used interchangeably and refer to the deposition of any amount of energy in a target cell nucleus by the passage of a single alpha-particle track through a portion of that target.) Thus, it would be useful, perhaps almost essential, for the biologist or oncologist to have a realistic concept of the spread (s.d.) of dose values that the individual targets may accumulate. Equally essential is an estimate of the probability that a target may not be hit at all or may be hit by less than a specified number of alpha particles. Here, we propose a practical means for calculating those parameters that are necessary for alpha-particle dosimetry.

There are two dosimetric systems that have been applied for alpha particles. The MIRD system relates the absorbed dose for a particular target to a given source distribution (*15*). Recently, Goddu et al. (*16,17*) applied this system in calculating the absorbed dose to the cell nucleus for various source configurations. The MIRD schema provides an average dose to the cell nucleus, which may be appropriate at large doses of alpha particles. However, this approach may have limited applicability at low doses particularly when a fraction of targets are not intersected by alpha-particle tracks.

A second system, microdosimetry, considers the stochastic variations of the energy deposited within small targets. As such, the result is not a single value of the energy deposited per unit mass. Rather, there is a distribution of specific energy, z (the microdosimetric analog of absorbed dose). Although two different specific-energy distributions may have the same average dose, they can result in significantly different levels of cell killing (or levels of some other biological endpoint) (*18*). Thus, microdosimetry is important because it is important in therapeutic applications to understand the cellular response to alpha particles. The disadvantage of microdosimetry is that the determination of such a distribution is often computationally intensive.

There are two approaches for calculating microdosimetric specific-energy distributions, f(z), for alpha particles [where f(z) dz is the fraction of depositions for which the specific energy is between z and z + dz]. One approach uses Monte Carlo methods (*18–22*), which require a large number of simulations to achieve a good statistical representation. In the second approach, the single-event distribution (which represents the distribution of specific energy for exactly one alpha particle intersecting the target) is convolved using transforms to determine the multihit distribution (*23–27*). This approach is efficient for simple source configurations, but is cumbersome for complex source arrangements.

The determination of a complete microdosimetric distribution of specific energies for all the different source–target configurations is an impractical means of achieving the needed information. It is much simpler to use the MIRD schema and build on it. Two additional quantities are tabulated along with the MIRD S-factors for each separate source–target pair. These are the first and second moments of the single-hit specific-energy distributions, $\langle z_1 \rangle$ and $\langle z_1^2 \rangle$. We describe here how these two quantities suffice to give estimates of the s.d. and the probability of zero hits (or any other number) for any combination of sources producing alpha particles that can reach the target. In

Received Sep. 16, 1996; revision accepted Mar. 4, 1997.

For correspondence or reprints contact: John C. Roeske, PhD, Department of Radiation and Cellular Oncology, The University of Chicago, MC 9006, 5758 South Maryland Avenue, Chicago, IL 60637.

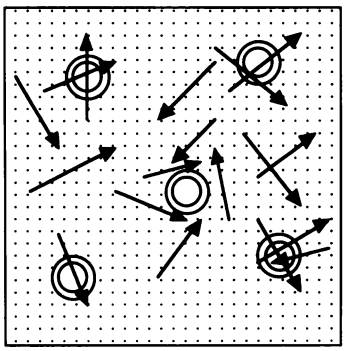

FIGURE 1. Schematic diagram illustrating the necessity for dosimetric information in addition to the average dose. Note that, although some cells receive multiple-hits from alpha-particle emissions, a fraction of the cells may receive few, if any, hits.

addition, this extension to the MIRD schema is clarified through the use of a simple example.

MATERIALS AND METHODS

The microdosimetric principles on which these methods are based have been described in detail by Kellerer (*28*) and by Roesch (*29*). This discussion is divided into two sections. The first section examines the relationship between the single-hit specific-energy distribution, $f_1(z_1)$ and the multihit specific-energy distribution, f(z). The second section demonstrates how the total multihit specific-energy distribution for several sources is related to the distributions for each separate source.

Single-Hit and Multihit Specific-Energy Distributions

There are two general methods for calculating single-event energy depositions. One, originated by Caswell (*30*), is applicable for any shape target for which the chord-length distribution is known. However, it requires a uniform distribution of sources over the volume from which the particles can reach the target. The other, described by Stinchcomb and Roeske (*26*), requires a spherical target shape, but is applicable for any nonuniform distribution of source radionuclides. The distribution in energies deposited by a single transit is transformed into the single-hit specific-energy distribution by using the relation:

$$z_1 = \varepsilon/m, \qquad \text{Eq. 1}$$

where m is the mass of the target and ϵ is given by:

$$\varepsilon = \int_{t_1}^{t_2} (dE/dx)\, dx. \qquad \text{Eq. 2}$$

In Equation 2, dE/dx is the stopping power, and the limits of integration are over the residual range of the particle on entering and/or leaving the target. Several assumptions enter in the determination of this path. One is that the emission probability for the source radionuclide is isotropic. The second is that the alpha-particle traversal can be approximated by a straight line and that the continuous slowing down approximation can be used to calculate the energy deposition along this line. Thus, we assumed negligible scattering and statistical fluctuations in energy deposition for a given chord length. This approximation is valid for alpha particles having energies less than 10 MeV (*31*). In addition, the effects of delta rays and the width of the alpha track can be ignored because the targets we will be considering (>1 μm in diameter) are much larger than the ranges of the delta rays and the widths of the tracks (*31*).

When more than a single hit occurs, the multihit specific-energy distribution, f(z), is obtained by convolutions of the single-hit distribution, $f_1(z_1)$. For example, the distribution for two hits is:

$$f_2(z) = \int_0^\infty f_1(z_1)\, f_1(z - z_1)\, dz_1. \qquad \text{Eq. 3}$$

This convolution integral is evaluated by either Fourier or Laplace transforms using the theorem that the transform of the convolution is the product of the transforms of the functions convolved. Hence:

$$T_2 = T_1^2, \qquad \text{Eq. 4}$$

where T_1 and T_2 are the transforms of $f_1(z_1)$ and $f_2(z)$, respectively.

For exactly n hits, the distribution of specific energies, $f_n(z)$, is the n-fold convolution of the single-hit distribution, $f_1(z_1)$:

$$T_n = T_1^n, \qquad \text{Eq. 5}$$

where T_n is the transform of $f_n(z)$. These transforms (Laplace) can be written either as an integral over the corresponding distribution or as a summation over the moments of that distribution:

$$T = \int_0^\infty e^{-uz} f(z)\, dz = \sum_0^\infty \langle z_i \rangle (-u)^i/i!. \qquad \text{Eq. 6}$$

This summation results from expanding the exponential as a series of terms in increasing powers of uz and using the definitions of the moments:

$$\langle z^i \rangle = \int_0^\infty z^i f(z)\, dz. \qquad \text{Eq. 7}$$

Assuming a Poisson probability for n hits, given an average of $\langle n \rangle$ hits, one obtains the following theorem relating the transform, T, of the multihit distribution, f(z), to T_1:

$$T = \exp[\langle n \rangle (T_1 - 1)]. \qquad \text{Eq. 8}$$

This is a fundamental theorem in microdosimetry derived initially for external beam dosimetry. This same relation applies also to internal emitters provided that each individual emitter (nucleus or particulate) emits exactly one alpha particle rather than an average number with a Poisson distribution about this average (*26*).

After taking the logarithm of both sides of Equation 8, one can express ln (T) as a summation over powers of T − 1. Then, using Equation 6 to write the transforms in terms of the moments, one obtains a rather complicated identity in which both sides are functions of u. Equating the coefficients of the first power of u on both sides shows that:

$$\langle z \rangle = \langle n \rangle \langle z_1 \rangle. \qquad \text{Eq. 9a}$$

Because the average specific energy, $\langle z \rangle$, is the absorbed dose, D, this becomes:

$$D = \langle n \rangle \langle z_1 \rangle. \qquad \text{Eq. 9b}$$

Similarly, equating the coefficients of the second power gives:

$$\langle z^2 \rangle - \langle z \rangle^2 = \langle n \rangle \langle z_1^2 \rangle. \qquad \text{Eq. 10a}$$

Because the left side of this equation is the definition of the variance, σ^2, of the multihit distribution, this becomes:

$$\sigma^2 = \langle n \rangle \langle z_1^2 \rangle. \qquad \text{Eq. 10b}$$

Now it becomes evident that, if the values of the S-factor, $\langle z_1 \rangle$ and $\langle z_1^2 \rangle$ are all tabulated for a source–target pair and if the cumulated activity and the S-factor are used to give the absorbed dose in the usual MIRD formulation, then using Equation 9b, we can determine $\langle n \rangle$. This, in turn, is multiplied by $\langle z_1^2 \rangle$ to yield the

TABLE 1
Values of the S-Factor, $\langle z_1 \rangle$ and $\langle z_1^2 \rangle$ for Experimental Results of Azure et al. (*32*)*

	Alpha energy			
	8.78 MeV		6.05 MeV	
Parameter	Nucleus ← nucleus	Nucleus ← cytoplasm	Nucleus ← nucleus	Nucleus ← cytoplasm
S-factor (Gy/Bq · sec)	0.1065	0.0480	0.1416	0.0645
$\langle z_1 \rangle$ (Gy)	0.1065	0.1723	0.1416	0.2314
$\langle z_1^2 \rangle$ (Gy^2)	0.0162	0.0349	0.0287	0.0631

*Cell radius = 5 μm; nuclear radius = 4 μm.

variance and its square root, the s.d. Furthermore, using Poisson statistics, the probability that the target is not hit is simply exp $(-\langle n \rangle)$, and the probability that there are k hits or less is:

$$\exp(-\langle n \rangle)[1 + \langle n \rangle + \langle n \rangle^2/2 + \cdots + \langle n \rangle^k/k!]. \quad \text{Eq. 11}$$

Combining Multihit Distributions from Several Sources

When a target receives energy deposition from two different source configurations, A and B, the resulting specific energy distribution is the convolution of the separate specific energy distributions. For example, these sources may consist of activity distributed on the surface of the cell and activity outside of the cell. It follows that the transforms of these distributions multiply:

$$T = T_A T_B. \quad \text{Eq. 12}$$

Again using Equation 6 to write these transforms in terms of the moments of the specific-energy distributions, another identity in u results. Equating the coefficients of similar powers of u on both sides shows that:

$$\langle z \rangle = \langle z_A \rangle + \langle z_B \rangle \text{ or } D = D_A + D_B \quad \text{Eq. 13}$$

and

$$\langle z^2 \rangle = \langle z_A^2 \rangle + 2\langle z_A \rangle \langle z_B \rangle + \langle z_B^2 \rangle, \quad \text{Eq. 14}$$

or (using the definition of the variance, σ^2):

$$\sigma^2 = \sigma_A^2 + \sigma_B^2. \quad \text{Eq. 15}$$

Combining Equations 13 and 15 with Equations 9 and 10 yields:

$$D = \langle n \rangle \langle z_1 \rangle = \langle n_A \rangle \langle z_{1A} \rangle + \langle n_B \rangle \langle z_{1B} \rangle \quad \text{Eq. 16}$$

and

$$\sigma^2 = \langle n \rangle \langle z_1^2 \rangle = \langle n_A \rangle \langle z_{1A}^2 \rangle + \langle n_B \rangle \langle z_{1B}^2 \rangle, \quad \text{Eq. 17}$$

where

$$\langle n \rangle = \langle n_A \rangle + \langle n_B \rangle. \quad \text{Eq. 18}$$

These results can easily be extended from two unique source distributions to a complex array of sources. In summary, the dose and the average number of hits are summed over several sources, whereas the first and second moments of the single-hit specific-energy distribution are averaged over the several sources weighted by the average number of hits from each source.

RESULTS

The goal of this work was to develop a dosimetric framework for analyzing the biological results from therapeutic alpha-particle emitters. As such, we have identified three parameters that are potentially useful for clinicians and radiobiologists in evaluating the biological response to alpha-particle irradiation. These parameters are:

1. average dose;
2. s.d. of the multihit specific-energy spectrum; and
3. fraction of cells receiving zero (or any particular number of) hits.

Using the MIRD approach, the cumulated activity was determined in each compartment and multiplied by the appropriate S-factor to determine the average dose. The average number of hits from a source within a given compartment was determined by dividing the absorbed dose from that source by the corresponding value of the first moment of the single-event spectrum. The average number of hits from a complex source configuration was then the sum of the hits from each compartment. To calculate the variance, the mean number of hits from each source compartment was multiplied by the corresponding value of the second moment of the single-event spectrum and summed to yield the total variance.

To clarify the use of this method, we considered the following example, based on an experiment by Azure et al. (*32*). The details of this experiment have been described previously (*32,33*) and will be described here only briefly. The purpose of their investigation was to determine the radiotoxicity of ^{212}Pb in Chinese hamster lung fibroblasts (V79-513 cells). Using various concentrations of dipyrrolidinedithiocarbamato-^{212}Pb(II), uptake experiments were performed to assess the incorporation of this compound as a function of time and initial activity. Additional data were obtained to determine the subcellular distribution of activity (i.e., nucleus compared to cytoplasm). Here, we report a mean lethal cumulated activity (defined as the cumulated activity required to reduce the surviving fraction to 0.37) of 10.8 Bq · sec, of which 72% is contained in the nucleus and 28% in the cytoplasm (both distributions are assumed to be Poisson and uniform). Based on this source data, the goal was to calculate the absorbed dose, s.d. and fraction of cells receiving no hits.

In this example, we assumed that the critical target is the cell nucleus (radius = 4 μm). Sources were assumed to be distributed randomly and uniformly (but with different concentrations) in the nucleus and in the cytoplasm (cell radius = 5 μm) (*32*). The S-factors and values of $\langle z_1 \rangle$ and $\langle z_1^2 \rangle$ were calculated for alpha particles emitted from ^{212}Pb daughters: 64% of the alpha particles had an energy of 8.78 MeV, and 36% had an energy of 6.05 MeV. The source–target pairs were nucleus ← nucleus and nucleus ← cytoplasm. The calculations used stopping power and range data contained in ICRU Report 49 for water (*34*) and followed the analytic method outlined previously (*26*). Note that the beta and gamma emissions were neglected in this calculation because the dose contributed by these was expected to be much less than the alpha-particle component.

Table 1 shows the resulting values of the S-factors, $\langle z_1 \rangle$ and $\langle z_1^2 \rangle$. Figures 2 and 3 show the single-hit specific-energy distributions for 8.78-MeV alpha particles emitted in the nu-

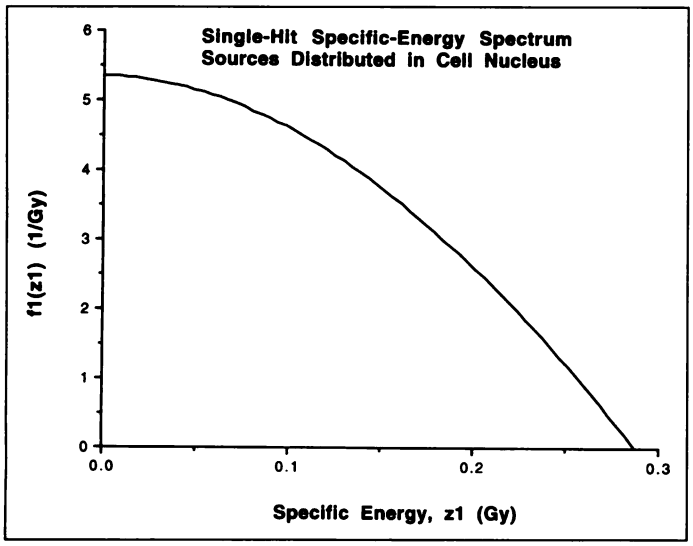

FIGURE 2. The single-hit specific-energy distribution in a target cell nucleus that is 4 μm in radius for a uniform source of 8.78-MeV alpha particles throughout the same nucleus. The average specific energy for this distribution is 0.1065 Gy, and the variance is 0.0162 Gy^2.

cleus and in the cytoplasm, respectively. The distributions for the 6.05-MeV alpha particle are very similar in shape and are not shown. Note that the energy deposited by the recoil nuclei from alpha-particle decay is not included in Table 1 or in Figure 2.

Of particular interest is the shape of these spectra. In both figures, the maximum specific energy corresponds to a single alpha particle traversing the diameter of the spherical nucleus. The maximum values are approximately the same regardless of whether the emission occurs within the nucleus or the cytoplasm because the LET is relatively constant over the distance traversed by the 8.78-MeV alpha particle. Although the maximum energy may be the same, the spectra are significantly different. When the alpha particle is emitted within the cell nucleus, all paths are starters. The probability of the particle traversing short distances (depositing only small amounts of energy) before leaving the nucleus is higher than the probability of it traveling large distances (depositing large amounts of energy) in an equivalent interval of specific energy dz_1. Thus, the maximum in the distribution in Figure 2 occurs at nearly zero specific energy and decreases as the specific energy increases in value. However, when the alpha-particle decay occurs in the cytoplasm, all paths through the nucleus are crossers. Thus, the number of paths depositing a specific energy within a given interval near the maximum specific energy is larger than the number depositing a specific energy within an equivalent interval near zero specific energy. Thus, the distribution in Figure 3 has its maximum at nearly the maximum specific energy and decreases as the specific energy decreases to zero. Note that the shapes of these curves are somewhat similar to the shapes of the chord length distributions through a spherical target for the two cases because the LET is nearly constant. A more detailed discussion of these chord-length distributions can be found in Eckerman et al. (*35*).

Table 2 illustrates how the values from Table 1 are easily combined to give the absorbed dose, its s.d. and the probability of no hits based on the value of the mean lethal cumulated activity. The computation of the total dose proceeds as a typical MIRD calculation; i.e., the cumulated activity for each source–target pair is multiplied by the corresponding S-factor to give the partial doses, which are then added. The number of hits for each source–target pair for each alpha-particle energy is obtained by dividing the partial dose for that pair by the value of $\langle z_1 \rangle$ for that pair. Then, the number of hits for all of the sources is added to get the total number of hits, $\langle n \rangle$. The probability that an individual target receives no hits is $\exp(-\langle n \rangle)$. The variance in the partial dose from each of the sources is obtained by multiplying the number of hits from that source–target pair by the corresponding value of $\langle z_1^2 \rangle$. These variances are then added to get the variance of the multihit specific-energy spectrum, σ^2. The results of this simple example show that the average dose delivered to the cell nucleus is 1.09 Gy, with a s.d. of the multihit specific-energy distribution equal to 0.45 Gy. The average number of hits to the cell nucleus is 8.62, resulting in a fraction of cells receiving zero hits equal to 1.8×10^{-4}. Consider if the cumulated activity were only one-tenth of the experimental value (i.e., 1.08 Bq · s). The corresponding doses and average numbers of hits are reduced by a factor of 10, and the s.d. is reduced by a factor of $\sqrt{10}$ of the former values. Additionally, there is a considerable increase in the probability of no cells receiving hits.

Although not needed for the computations, Figures 4 and 5 show the multihit specific-energy distributions for this example using these two values of cumulated activity (10.8 Bq · sec and 1.08 Bq · sec, respectively). Note that, in Figure 4, the multihit specific-energy distribution is nearly Gaussian in shape. For cases where the average number of hits is relatively large, the central limit theorem predicts that the multihit spectrum will approach a Gaussian in shape. Hence, the mean dose and the s.d. are sufficient to describe the entire spectrum. In general, the spectrum can be approximated by a Gaussian function when the s.d. is less than approximately 20% of the average dose. However, as the mean number of hits decreases, the specific-energy spectrum becomes skewed (e.g., Fig. 5) as a larger fraction of cells receive zero hits. In both cases, the specific-energy distribution demonstrates the need for providing information in addition to the average dose.

Consider an example in which the total cumulated activity is increased to give a surviving fraction of only 10^{-8} instead of

TABLE 2
Calculation of Average Dose, s.d. and the Fraction of Cells Receiving Zero Hits*

	Alpha energy				
	8.78 MeV		6.05 MeV		
Parameter	Nucleus ← nucleus	Nucleus ← cytoplasm	Nucleus ← nucleus	Nucleus ← cytoplasm	Total
Cumulated activity (Bq · sec)	4.98	1.93	2.80	1.09	10.8
Average dose (Gy)	$4.98 \times 0.1065 = 0.530$	$1.93 \times 0.0480 = 0.093$	$2.80 \times 0.1416 = 0.396$	$1.09 \times 0.0645 = 0.070$	1.089
Average no. of hits	0.530/0.1065 = 4.98	0.093/0.1723 = 0.54	0.396/0.1416 = 2.80	0.070/0.2314 = 0.30	8.62
σ^2, dose variance (Gy^2)	$4.98 \times 0.0162 = 0.081$	$0.54 \times 0.0349 = 0.019$	$2.80 \times 0.0287 = 0.080$	$0.30 \times 0.0631 = 0.019$	0.199

*s.d. in total dose: $\sqrt{0.199} = 0.45$ Gy; total average dose to a cell nucleus: 1.09 ± 0.45 Gy; probability that a nucleus is not hit: $e^{-8.62} = 1.8 \times 10^{-4}$.

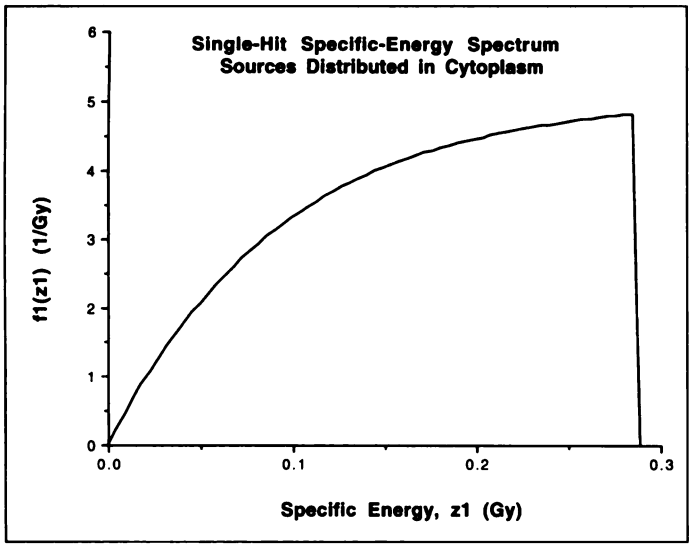

FIGURE 3. The single-hit specific-energy distribution in a target cell nucleus that is 4 μm in radius for a uniform source of 8.78-MeV alpha particles throughout the cytoplasm surrounding this nucleus, in a cell of radius 5 μm. The average specific energy for this distribution is 0.1723 Gy, and the variance is 0.0349 Gy^2.

0.37. This requires an increase in the cumulative activity by a factor of 8 × 2.3 = 18.4 because 10 = exp (2.3). All the quantities in the right ("Total") column of Table 2 increase by the same factor, 18.4. Thus, the dose is increased to 18.4 × 1.089 = 20 Gy. The variance is also increased by a factor of 18.4, and the relative variance is reduced by the same factor from 17% to slightly less than 1%. This reduces the relative s.d. from 41% to slightly less than 10%, which is relatively insignificant. The average number of hits, ⟨n⟩, increases to 8.62 × 18.4 = 158.6. Thus, the fraction of cells not hit is negligible.

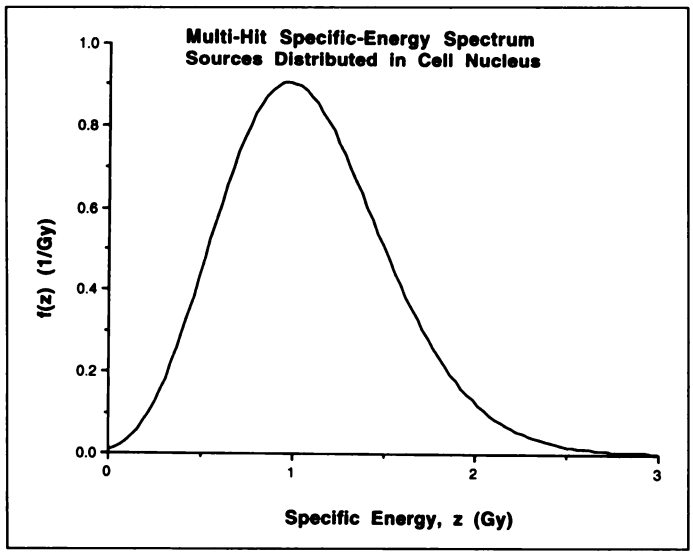

FIGURE 4. The multihit specific-energy distribution in a target cell nucleus that is 4 μm in radius centered in a cell of radius 5 μm for a ^{212}Pb source, containing 10.8 Bq · sec cumulated activity per cell, of which 72% is contained uniformly in the nucleus and 28% is in the cytoplasm. Of the ^{212}Pb decays, 64% emit 8.78-MeV alpha particles, and 36% emit 6.05-MeV alpha particles. The average specific energy (dose) of 1.09 Gy and its s.d. of 0.45 Gy are obtained simply, without knowledge of this multihit distribution (see Table 2). The area under the curve is 0.99982, allowing for a delta function of area 0.00018 (also obtained simply), representing the fraction of such nuclei that are not hit.

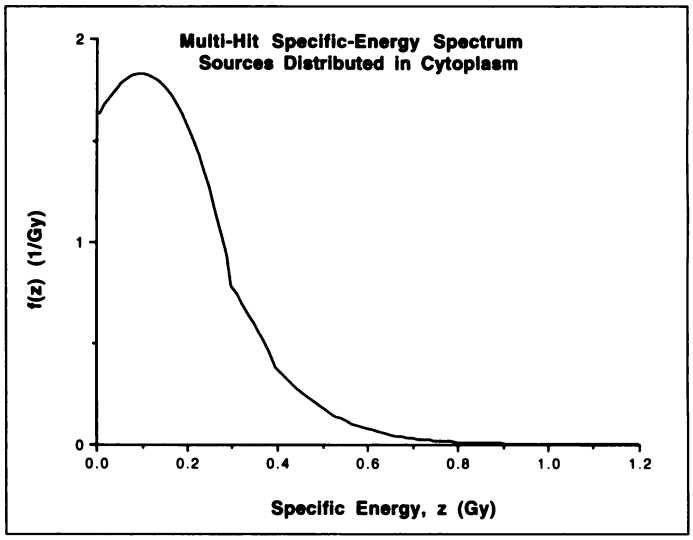

FIGURE 5. The multihit specific-energy distribution for the same source–target configuration that was described in Figure 4, except that cumulated activity is reduced by a factor of 10 (1.08 Bq · sec per cell). The average specific energy (dose) of 0.109 Gy and its s.d. of 0.14 Gy are obtained simply, without knowledge of this multihit distribution (see Table 2). The area under the curve is 0.58 allowing for a delta function (data not shown) of area 0.42, representing the fraction of such nuclei that are not hit.

DISCUSSION

Here, we have described a dosimetry system that includes the computational ease of MIRD and the detailed information from microdosimetry. In addition to the standard S-factors, we have proposed the tabulation of the first and second moments of the single-event specific-energy spectrum. These parameters may be used in conjunction with the S-factor to calculate the s.d. and the average number of hits to a spherical cell nucleus exposed to a given radiation field. The average number of hits may, in turn, be used with the Poisson distribution to calculate the fraction of cells receiving any number of hits. It is expected that this additional information, along with the average dose, will aid in the interpretation of radiobiological studies and clinical outcomes with therapeutic alpha-particle emitters.

As with any dose calculation scheme for internal emitters, the accuracy of the calculation is limited by the ability to quantify activity within a given organ in vivo. Information on the activity distribution may be gained through nuclear medicine imaging studies. In many cases, this may provide an adequate estimate of the nonspecific background activity, but may have limited applicability for tumor activity. Because alpha-particle emitters will be most effective in disease involving from 1 cell to 10^7 cells, it is expected that the activity in the target tissue will be beyond the resolving capabilities of most systems. However, through modeling and animal data, it is possible to calculate these parameters to determine if the activity delivered is capable of providing a therapeutically favorable effect. For example, it would be critical to know if a fraction of the tumor cells are receiving no dose whatsoever. Additionally, the use of this system in estimating dose parameters for normal tissues is equally important for dose-limiting structures, such as bone marrow.

One of the advantages of using this method is that the dosimetric parameters that are associated with complex source configurations can be tabulated by summing the contributions of each individual component. For example, if a source consists of different quantities of activity in the cell nucleus, in the cytoplasm, on the cell surface and outside of the cell, the average dose is simply the sum of the product of the S-factors and the activity associated with each compartment. The same

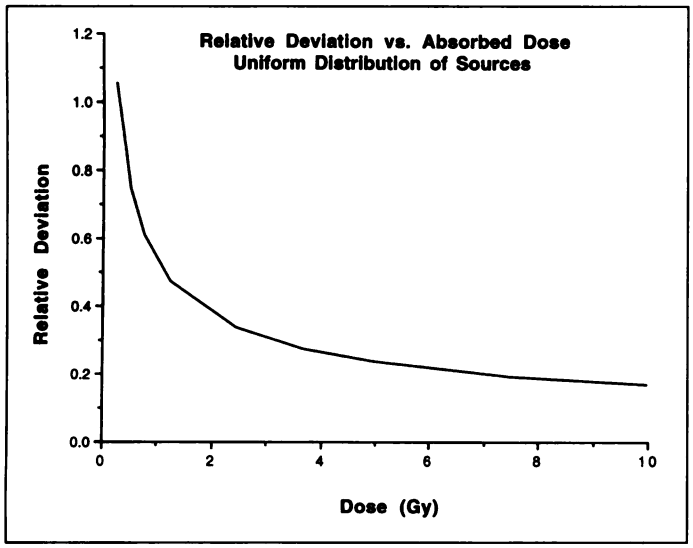

FIGURE 6. The relative deviation as a function of absorbed dose to a 10-μm spherical cell nucleus irradiated in a uniform solution of ^{212}Bi. At low doses, the relative deviation is high decreasing to approximately 20% of the mean absorbed dose at 7 Gy. Note, the relative deviation is inversely proportional to the square root of the absorbed dose.

approach, as described in Equations 13–18, can be applied to determine the s.d. and the average number of hits of this distribution. This is much simpler than the Monte Carlo approach, in which this complex source configuration would need to be simulated 10,000–100,000 times to achieve reasonable statistics.

A question that arises is: When is it appropriate to use the MIRD schema instead of microdosimetry for alpha particles? An answer to this question is suggested by ICRU Report 36 on Microdosimetry (*36*). Here, it is stated that the statistical fluctuation in energy deposition is relatively insignificant for a high absorbed dose, in which the relative s.d. of the frequency mean specific energy is less than 20%, and that this borderline distinguishes macrodosimetry from microdosimetry. Thus, the exact dose for which this occurs will be a function of the source configuration and the target size. Consider, for example, a 10-μm-diameter spherical cell nucleus irradiated in a uniform solution of ^{212}Bi. Shown in Figure 6 is the relative deviation compared to the absorbed dose to the target. At low doses, the deviations are large, decreasing to approximately 20% of the mean absorbed dose (1.4 Gy) at 7 Gy. At doses beyond this value, the relative deviation decreases less rapidly. Thus, it is recommended that, for a particular source–target configuration, the mean dose, s.d. and fraction receiving zero hits be calculated using the methods presented here. If the fraction of targets receiving zero hits is relatively small (e.g., <1%) and the s.d. is relatively small (e.g., <20% of the mean absorbed dose), a microdosimetric calculation may not be necessary.

In this preliminary analysis, we have presented a simplified example for a specific source–target configuration. However, there are other geometries that are required for clinical applications. Some geometries appropriate for tabulation of these quantities include:

1. cells in uniform distribution of alpha-particle emitters;
2. clusters of cells with activity localized on the surface, within the cytoplasm or in the cell nucleus;
3. a planar distribution of activity with a target cell located at various distances from the plane;
4. an interface with uniform activity on one side and zero (or different) activity on the other, with a target cell located at various distances from the interface; and
5. geometries that are appropriate to bone marrow.

In addition, it may be useful to investigate different idealized tissue geometries such as a closed-pack hexagonal arrangement of cells. These factors should be calculated for those radionuclides most likely to be used for therapy including ^{211}At, ^{212}Bi and ^{213}Bi. In addition, it may be useful to calculate tables for particular source energies ranging from 3 MeV to 10 MeV. This allows dosimetric parameters to be readily determined for new radionuclides or for cases where the daughter products are relatively long-lived, such that translocation is an issue.

CONCLUSION

For alpha particles intersecting targets of cellular dimensions, the MIRD schema is applied with the addition of the values of the first and second moments of the single-hit specific-energy distributions, $\langle z_1 \rangle$ and $\langle z_1^2 \rangle$ for each source–target pair. This allows one to easily obtain not only the absorbed dose to the target but also the spread (s.d.) of dose values that the individual targets may receive. In addition, it allows an estimate of the probability that a target may not be hit at all or that it may be hit by less than a specified number of alpha particles. Consequently, a complete microdosimetric analysis involving the calculation of the multihit specific-energy distribution is not necessary to obtain this information. An example shows the simplicity of the computations. Tables that include these first and second moments along with the S-factors are being prepared for source–target pairs and for the alpha-particle energies that are most likely to be encountered with internal alpha-particle therapy.

REFERENCES

1. Rotmensch J, Atcher RW, Hines J, et al. The development of alpha-emitting radionuclide lead-212 for the potential treatment of ovarian carcinoma. *Am J Obstet Gynecol* 1989;160:789–797.
2. Rotmensch J, Atcher RW, Schlenker R, et al. The effect of alpha-emitting radionuclide lead 212 on human ovarian carcinoma: a potential new form of therapy. *Gynecol Oncol* 1989;32:236–239.
3. Rotmensch J, Atcher RW, Hines J, Toohill M, Herbst AL. Comparison of short-lived high-LET alpha-emitting radionuclide lead-212 and bismuth-212 to low-LET x-rays on ovarian carcinoma. *Gynecol Oncol* 1989;35:297–300.
4. Macklis RM, Kaplan WD, Ferrara JLM, et al. Alpha particle radioimmunotherapy: animal models and clinical perspectives. *Int J Radiat Oncol Biol Phys* 1988;16:1377–1387.
5. Macklis RM, Kinsey BM, Kassis AI, et al. Radioimmunotherapy with alpha-particle-emitting immunoconjugates. *Science* 1988;240:1024–1026.
6. Kozak RW, Atcher RW, Gansow OA, Friedman AM, Hines JJ, Waldman TA. Bismuth-212-labeled anti-TAC monoclonal antibody: alpha-particle-emitting radionuclides as modalities for radioimmunotherapy. *Proc Natl Acad Sci USA* 1986;83:474–478.
7. Kurtzman SH, Russo A, Mitchell JB, et al. Bismuth-212 linked to an antipancreatic carcinoma antibody: model for alpha-particle-emitter radioimmunotherapy. *J Natl Cancer Inst* 1988;80:449–452.
8. Junghans RP, Dobbs D, Brechbiel MW, et al. Pharmacokinetics and bioactivity of 1,4,7,10-tetra-azacylododecane off',N'',N'''-tetraacetic acid (DOTA)-bismuth-conjugated anti-Tac antibody for alpha-emitter (^{212}Bi) therapy. *Cancer Res* 1993;53:5683–5689.
9. Palayoor ST, Humm JL, Atcher RW, Hines JJ, Macklis RM. G_2-M arrest and apoptosis in murine T lymphoma cells following exposure to ^{212}Bi alpha particle irradiation. *Nucl Med Biol* 1993;20:795–805.
10. Geerlings MW, Kaspersen FM, Apostolidis C, van der Hout R. The feasibility of 225Ac as a source of alpha-particles in radioimmunotherapy. *Nucl Med Commun* 1993;14:121–125.
11. Macklis RM, Lin JY, Beresford B, Atcher RW, Hines JJ, Humm JL. Cellular kinetics, dosimetry, and radiobiology of alpha-particle radioimmunotherapy: induction of apoptosis. *Radiat Res* 1992;130:220–226.
12. Rotmensch J, Schwartz JL, Atcher RW, Harper PV, DeSombre E. Increased nuclear damage by high linear energy transfer radioisotopes applicable for radiodirected therapy against radiologic malignancies. *Gynecol Obstet Invest* 1991;32:180–184.
13. Hall EJ. *Radiobiology for the radiologist*, 2nd Ed. Hagerstown, MD: Harper and Row; 1978:65–77.
14. Polig, E. Localized alpha-dosimetry. In: Ebert M, Howards A, eds. *Current topics in radiation research*, Vol. 13. Amsterdam: North Holland; 1978:189–327.

15. Loevinger R, Budinger TF, Watson EE. *MIRD primer for absorbed dose calculations*, Revised. New York: The Society of Nuclear Medicine; 1991:1-22.
16. Goddu SM, Howell RW, Rao DV. Cellular dosimetry: absorbed fractions for monoenergetic electron and alpha-particle sources and S-values for radionuclides uniformly distributed in different cell compartments. *J Nucl Med* 1994;35:303–316.
17. Goddu SM, Howell RW, Buchet LG, Bolch WE, Rao D. MIRD cellular S values: self-absorbed dose per unit cumulated activity for selected radionuclides and monoenergetic electron and alpha particle emitters incorporated into different cell compartments. Reston, VA: The Society of Nuclear Medicine; 1997:2-14.
18. Humm JL. A microdosimetric model of astatine-211 labelled antibodies for radioimmunotherapy. *Int J Radiat Oncol Biol Phys* 1987;13:1767–1773.
19. Humm JL, Chin LM. A model of cell inactivation by alpha-particle internal emitters. *Radiat Res* 1993;134:143–150.
20. Charlton DE, Sephton R. A relationship between microdosimetric spectra and cell survival for high-LET irradiation. *Int J Radiat Biol* 1991;59:447–457.
21. Charlton DE, Kassis AI, Adelstein SJ. A comparison of experimental and calculated survival curves for V79 cells grown as monolayers or in suspension exposed to alpha irradiation from 212-Bi distributed in the growth medium. *Radiat Prot Dosim* 1994;52:311–315.
22. Humm JL, Roeske JC, Fisher DR, Chen GTY. Microdosimetric concepts in radioimmunotherapy. *Med Phys* 1993;20:535–541.
23. Roesch WC. Microdosimetry of internal sources. *Radiat Res* 1977;70:494–510.
24. Fisher DR. The microdosimetry of monoclonal antibodies labeled with alpha emitters. In: Schlafke-Stelson AT, Watson EE, eds. *Proceedings of the fourth international radiopharmaceutical dosimetry symposium*. Oak Ridge, TN: Oak Ridge Associated Universities; 1986:26–36.
25. Fisher DR, Harty R. The microdosimetry of lymphocytes irradiated by alpha particles. *Int J Radiat Biol* 1982;41:315–324.
26. Stinchcomb TG, Roeske JC. Analytic microdosimetry for radioimmunotherapeutic alpha emitters. *Med Phys* 1992;19:1385–1393.
27. Stinchcomb TG, Roeske JC. Survival of alpha-particle irradiated cells as a function of the shape and size of the sensitive volume (nucleus). *Radiat Prot Dosim* 1995;62:157–164.
28. Kellerer AM. Analysis of patterns of energy deposition; a survey of theoretical relations in microdosimetry. In: Ebert HG, ed. *Proceedings of the second symposium on microdosimetry*. Brussels: Commission of European Communities: 1970:107–134.
29. Roesch WC. Moments of microdosimetric quantities for particulate sources. *Radiat Res* 1985;102:392–398.
30. Caswell RS. Deposition of energy by neutrons in spherical cavities. *Radiat Res* 1996;27:92–107.
31. Kellerer AM, Chmelevsky D. Criteria for the applicability of LET. *Radiat Res* 1975;63:226–234.
32. Azure MT, Archer RD, Sastry KSR, Rao DV, Howell RW. Biological effects of lead-212 localized in the nucleus of mammalian cells: role of recoil energy in the radiotoxicity of internal alpha-particle emitters. *Radiat Res* 1994;140:276–283.
33. Howell RW, Rao DV, Hou D-Y, Narra VR, Sastry KSR. The question of relative biological effectiveness and quality factor for Auger emitters incorporated into proliferating mammalian cells. *Radiat Res* 1991;128:282–292.
34. ICRU. *Stopping powers, ranges for protons, and alpha particles*, International Commission of Radiation Units and Measurements Report No. 49. Bethesda, MD: ICRU; 1993:256.
35. Eckerman KF, Ryman JC, Taner AC, Kerr GD. Traversals of cells by radiation and absorbed fraction estimates for electrons and alpha particles. In: A. T. Schlafke-Stelson and E. E. Watson, eds. *Proceedings of the fourth international radiopharmaceutical dosimetry symposium*. Oak Ridge, TN: Oak Ridge Associated Universities; 1986:67–86.
36. ICRU. *Microdosimetry*, International Commission of Radiation Units and Measurements Report No. 36. Bethesda, MD: ICRU; 1983:54–55.

D-Lysine Reduction of Indium-111 Octreotide and Yttrium-90 Octreotide Renal Uptake

Bert F. Bernard, Eric P. Krenning, Wout A.P. Breeman, Edgar J. Rolleman, Willem H. Bakker, Theo J. Visser, Helmut Mäcke and Marion de Jong

Departments of Nuclear Medicine and Internal Medicine III, Erasmus Medical University and Academic Hospital Dijkzigt, Rotterdam, The Netherlands; and Department of Nuclear Medicine, Kantonspital Basel, Basel, Switzerland

Indium-111-DTPA-octreotide (^{111}In-DTPAOC) is used successfully for imaging somatostatin receptor-positive lesions. A new and promising application is its use in peptide-receptor radionuclide therapy (PRRT). For the latter purpose, [DOTA^0,D-Phe^1,Tyr^3]octreotide (DOTATOC), which is suitable for stable radiolabeling with ^{90}Y, is probably even more promising. Significant renal uptake of these octreotide analogs exists, however, reducing the scintigraphic sensitivity for detection of small tumors in the perirenal region and limiting the possibilities for PRRT. We showed that the renal uptake of ^{111}In-DTPAOC could be reduced to about 50% of control by L-lysine administration in vivo in rats. This study compares the effects of several doses and different methods of administration of D- and L-lysine, in addition to time-related effects of D-lysine, on kidney uptake of ^{111}In-DTPAOC and ^{90}Y-DOTATOC. **Methods:** Male Wistar rats (200–250 g) were given ^{111}In-DTPAOC (0.2 MBq, 0.5 μg-0.5 mg intravenously, intraperitoneally or orally) in the presence or absence of D- or L-lysine. At 1, 4 or 24 hr, the rats were killed, and the organs were isolated and counted for radioactivity. In different experiments, male Wistar rats (200–250 g) were given ^{90}Y-DOTATOC (1 MBq, 0.5 μg intravenously) in the presence or absence of D-lysine. At 24 hr, the rats were killed, and the organs were isolated and counted for radioactivity. **Results:** Administration of D- or L-lysine in a single intravenous dose of 400 mg/kg, resulted in more than 50% inhibition of kidney uptake of ^{111}In-DTPAOC at all time points tested, independently of the mass of ^{111}In-DTPAOC used. Higher or repeated doses of lysine did not give a significantly higher percentage inhibition. D-lysine, given orally in a dose of 400 mg/kg at 30 or 15 min before ^{111}In-DTPAOC injection, resulted in 30% and 20% inhibition of kidney uptake, respectively. L-lysine, given orally 30 min before ^{111}In-DTPAOC administration, resulted in 30% inhibition as well. Inhibition of kidney uptake of ^{111}In-DTPAOC by L-lysine after intraperitoneal administration was 40%. After L-lysine administration, ^{111}In-DTPAOC was decreased in the kidneys and in somatostatin receptor-positive organs such as the pancreas and adrenal glands. In contrast, D-lysine did not have a significant effect on uptake in octreotide receptor-positive organs. Renal uptake of ^{90}Y-DOTATOC was reduced by 65% by intravenous D-lysine, whereas radioactivity in blood, pancreas and adrenal glands was not affected. **Conclusion:** D-lysine may be preferred to L-lysine for reduction of renal uptake of radioactivity during scintigraphy and PRRT because of its lower toxicity and because it should not interfere with the natural amino acid metabolic balance.

Key Words: indium-111-octreotide; yttrium-90-octreotide; renal tubular reuptake; D-lysine; L-lysine; peptide-receptor radiotherapy

J Nucl Med 1997; 38:1929–1933

Indium-111 pentetreotide is a radiopharmaceutical that binds to somatostatin receptors present in certain tissues. It is being used for scintigraphic imaging of somatostatin receptor-positive lesions such as gastrointestinal pancreatic tumors, neuroblastoma, pheochromocytoma, breast cancer, Hodgkin's lymphoma and small-cell lung cancer (*1–3*). A new, interesting area of application is PRRT. Promising results have been reported in humans (*4*). However, although it emits Auger electrons, ^{111}In is not an optimal nuclide for radiotherapy. A beta-particle-emitting isotope such as ^{90}Y (maximum beta energy 2.3 MeV, half-life 64 hr) is more suitable for this purpose. However, [^{90}Y-DTPA^0]octreotide is not stable resulting in hematopoietic toxicity in vivo as ^{90}Y escapes to the skeleton (*5,6*). We have

Received Aug. 5, 1996; accepted Dec. 10, 1996.

For correspondence or reprints contact: Marion de Jong, PhD, Department of Nuclear Medicine, Academic Hospital Rotterdam, 3015 GD Rotterdam, The Netherlands.